THE EIGHTH INTERNATIONAL CONFERENCE
FOR
MECHANICAL POWER ENGINEERING
ALEXANDRIA UNIVERSITY
Alexandria, Egypt April 27-29, 1993

NUMERICAL COMPUTATION OF TIME-DEPENDENT FREE CONVECTION IN TALL, SQUARE AND SHALLOW CAVITIES

Karam M. El-Shazly

Mech. Engng. Dept., Faculty of Engng., Shoubra, Zagazig University

Abstract

Nusselt number correlations are presented for tall, square and shallow cavities heated from one side and cooled from other side, while its horizontal surfaces are insulated. Transient and steady-state patterns of stream function and temperature are presented. Energy, continuity and momentum equations need suitable time step in order to reach steady-state solution. A two-dimensional time-dependent numerical computation method has been developed to determine laminar free convection in closed cavities. The transport equations are solved with the implicit method. The resulting implicit method remains stable up to a Rayleigh number of 10^{12}. A transformation relation is proposed for sufficiently accurate determination of thermal and hydrodynamic boundary layers near the vertical side walls in cavities.

1- INTRODUCTION

For many heat transfer problems the governing differential equations are too complicated to be solved by analytical techniques. Therefore, a detailed and sufficiently accurate description of the resulting temperature and velocity patterns can only be achieved by numerical computation. Well known examples are the heat waste of hot fluid through internal heat transfer processes in thermal energy storage systems, temperature equalization processes in air conditioning systems and seasonal temperature distributions in lakes due to eddy and thermal mixing processes (Moog [1]). Experimental investigations are usually restricted to the study of laboratory models whereby the similarity conditions are often hard to meet.

Therefore, for most advanced problems the only acceptable solution method is a numerical computational technique. The literatures on numerical computation methods has been rapidly expanding in recent years but very few of these methods are of moderate value as the convergence and stability criteria are not sufficiently satisfied in fluid problems with high Rayleigh numbers of 10^6 and more. If the convergence and stability criteria are fully satisfied, the time step and/or the mesh size becomes so small that the needed computation time is far beyond any reasonable limit. Hence, there is still a strong demand for fast numerical computation techniques which avoid these difficulties

A review of various numerical techniques has been given by Torrance [2], Roache [3], Patankar [4] and Bejan [5].

2-Mathematical Formulation

Neglecting the dissipation and pressure term in the energy equation one obtains, subject to the usual Boussinesq approximation, the governing equation for an incompressible fluid with constant properties (except density) (see e. g. [6])

$$\nabla U = 0, \tag{1}$$

$$\frac{dU}{dt} = -\frac{1}{\rho_0}\nabla p + \nu \nabla^2 U + g\frac{\rho_0 - \rho}{\rho}, \tag{2}$$

$$\frac{dT}{dt} = \alpha \nabla^2 T \tag{3}$$

The dimensionless equations (continuity, momentum and energy) after introducing stream function and vorticity are;

$$\Omega = -\nabla^2 \Psi \tag{4}$$

$$\frac{d\Omega}{d\tau} = Pr \cdot \nabla^2 \Omega + Ra \cdot Pr \cdot \frac{\partial \Theta}{\partial X} \tag{5}$$

$$\frac{d\Theta}{d\tau} = \nabla^2 \Theta \tag{6}$$

Equations (4)-(6) are governing differential equations for free convection problems. To solve this set of equations is not a simple matter as the vorticity equation is coupled to the elliptic Poisson equation through the nonlinear convection terms.

Cavities heated from the side are primarily focused. This is due to the fact that the current applications in thermal insulation engineering, solar technology, rotating fluid machinery and energy management in architectural design are important class of flows.

A closed two-dimensional box which contains a Newtonian fluid is considered, and is shown schematically in Fig. 1. The side walls are held at different but uniform temperatures T_h and T_c. The top and bottom surfaces are insulated, and all surfaces are rigid non-slip boundaries.

The initial conditions are taken as:

$$\Theta(X,Y,0) = 0.5\ ,\quad U(X,Y,0) = V(X,Y,0) = \Psi(X,Y,0) = \Omega(X,Y,0) = 0 \tag{7}$$

The boundary conditions are

$$\Theta(0,Y,\tau) = 1\ ,\ \Theta(1,Y,\tau) = 0\ ,\quad \frac{\partial\Theta}{\partial Y}(X,0,\tau) = 0\ ,\quad \frac{\partial\Theta}{\partial Y}(X,1,\tau) = 0\ ,$$

$$U(0,Y,\tau) = U(X,0,\tau) = V(1,Y,\tau) = V(X,1,\tau) = 0 \tag{8}$$

For a numerical solution procedure these equations are usually directly transformed into finite difference equations with the aid of a proper differencing scheme. But to account for the vertical boundary layers near the side walls one would have to introduce an extremely dense grid which leads to a tremendous number of equations having to be solved. Generally, this situation can be improved either by mapping the flow area under consideration with a non-equidistance grid, i.e.

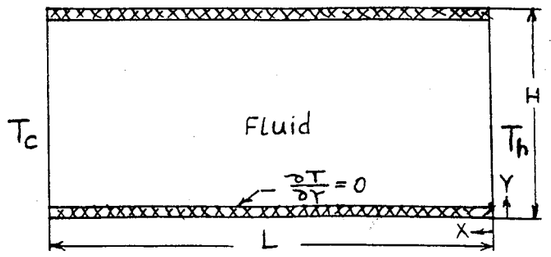

Fig.(1): Physical model of the system

small mesh size in the boundary region and larger grid distances in the core flow region or by introducing suitable transformation equations, r(x) and q(x), which accumulate the grid points in the boundary layer region.

3- Numerical Procedure

3-1 Energy, Vorticity and Stream function equations

The implicit method is the best known and widely used for transient solution. Application of implicit methods to two-dimensional problems, leads to a set of equations which can be solved by inversion of the resulting pentagonal matrix. The ADI-method (Alternating Directional Implicit method) by Peaceman and Rachford [7] splits the time step to obtain a multidimensional implicit method which requires only the inversion of a tridiagonal matrix. This tridiagonal matrix can be solved with the Gaussian elimination procedure.

The various iteration methods are very easy to understand and program. They are quite flexible, and are much faster than the direct methods in computational time. The 'Successive Overrelaxation' (SOR) method is the most popular of the iterative methods for solving Poisson equation in computational fluid dynamic problems. Implicit methods have become more popular in recent years. The procedure is to rewrite the elliptic equation as a time dependant equation as:

$$\frac{\partial \Psi}{\partial \tau} = \frac{\partial^2 \Psi}{\partial X^2} + \frac{\partial^2 \Psi}{\partial Y^2} + \Omega \tag{9}$$

One can write the energy, vorticity and stream function equations with using dummy variable Γ and transformation coordinates as:

$$\frac{\partial \Gamma}{\partial \tau} + a\left(A_x \cdot U \cdot \frac{\partial \Gamma}{\partial r} + A_y \cdot V \cdot \frac{\partial \Gamma}{\partial q}\right)$$

$$= b\left(A_x^2 \cdot \frac{\partial^2 \Gamma}{\partial r^2} + A_y^2 \cdot \frac{\partial^2 \Gamma}{\partial q^2} + B_x \frac{\partial \Gamma}{\partial r} + B_y \frac{\partial \Gamma}{\partial q}\right) + c \tag{10}$$

with $\left.\begin{matrix} a=1 \\ b=1 \\ c=0 \end{matrix}\right\}$ for energy equation, $\left.\begin{matrix} a=1 \\ b=Pr \\ c=Ra.Pr.A_x \frac{\partial \Theta}{\partial r} \end{matrix}\right\}$ for vorticity equation

and $\left.\begin{matrix} a=0 \\ b=1 \\ c=\Omega \end{matrix}\right\}$ for stream function equation. Dummy variable may be Θ for energy equation, Ω for vorticity equation and Ψ for stream function equation.

The nonlinear convective terms cause the main difficulties in separation in order to achieve a stable numerical method. This can be overcome by using the second-upwind-differencing-method.

The velocities are calculated by four points noncentral difference form. For Example, for the U velocity is

$$U(j,i) = \frac{\Psi(j-2,i) - 8\,\Psi(j-1,i) + 8\,\Psi(j+1,i) - \Psi(j+2,i)}{12\,\Delta q} \cdot A_x \tag{11}$$

The local Nusselt number is computed using a three points forward (or backward) approximation as

$$Nu = \frac{-3\,\Theta_0 + 4\,\Theta_1 - \Theta_2}{2\,\Delta r} \cdot A_x \tag{12}$$

Since the boundary conditions of the vorticity transport equation are not known it is necessary to determine the value of vorticities by using the second-order form as

$$\Omega_0 = \frac{-8\,(\Psi_1 - \Psi_2)}{2\,\Delta(r \text{ or } q)^2} \tag{13}$$

3-2 Stability and Accuracy of the Numerical Solutions

Unfortunately, a generally valid answer to what is the largest possible size that preserves numerical stability and yields acceptable accuracy does not exist. Since the answer depends not only on the individual problem but also on the individual problems solver. Plotting an overall result (such as the overall Nusselt number) versus grid size as shown in Fig. 2 is an effective way to visualize the range of ($\Delta r_x \Delta q$) values where the grid has become fine enough, that is, the range beyond which further decreases in Δr and Δq do not yield significant changes in the overall result. The time step $\Delta\tau$ and the mesh sizes Δr and Δq have to be chosen in such a way that all coefficients of the finite difference equation are positive and that the principal diagonal is still dominant. The stability condition is satisfied by introducing the second upwind differencing method.

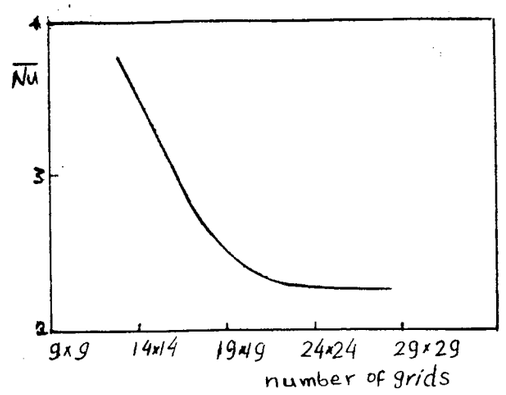

Fig.(2): Effect of grid spacing on the average Nusselt number; (pr=0.71 , A=1, $Ra=10^4$).

The coefficients of the finite difference equation become positive for the numerical scheme to be stable, the following condition must be satisfied

$$\Delta\tau \le \frac{1}{\frac{(U_r+fU_r! - U_l+fU_l!)}{2\,\Delta r} + \frac{(V_r + fV_r! - V_l + fV_l!)}{2\,\Delta q} + \left(\frac{C_1}{\Delta r^2} + \frac{C_2}{\Delta q^2}\right)} \qquad (14)$$

Where $C_1 = b \cdot A_x^2$ and $C_2 = b \cdot A_y^2$

Computational time step is a more important parameter which affects the results. Energy, vorticity and stream function equations may have time step at each node. The time-step value which, calculated from Eq. 14, depends on the left and right velocities at each node as well as the values of C_1 and C_2(i.e. the first derivative A_x and A_y which equal $\frac{\partial r}{\partial X}$ and $\frac{\partial q}{\partial Y}$ respectively change the values of time step).

The convergence criterion required for the solutions of the stream function was $\epsilon < 0.001$, more iterations for the stream function to converge will be made and the total computer time required increased.

Although exact solutions of the problem do not appear feasible, it is possible to determine approximately what magnitude error can be expected in the numerical solutions. The errors and the approximate solutions for the reference points can be estimated if numerical solutions with three different mesh sizes are known.

If one has numerical solutions G_k at each point (r_i , q_j) for different mesh sizes, one can write equations by neglecting higher order terms. The equations are:

$$G_{app} = G_1 + B\,h_1^n \qquad (15a)$$
$$G_{app} = G_2 + B\,h_2^n \qquad (15b)$$
$$G_{app} = G_3 + B\,h_3^n \qquad (15c)$$

where h_1, h_2 and h_3 are different mesh sizes. These values can be chosen as:

Grid	7 X 7	13X13	25X25
$1/h_k$	0.166	0.0833	0.0416

with $R = h_{k+1} / h_k = 0.5$, k=1,2 . One can write $h_2 = R \chi h_1$ and has three equations with three unknowns (G_{app}, B and n). The solutions are found by solving Eqs. (15a through 15c) and the results are :

$$n = \ln\left\{\frac{(G_3 - G_2)}{(G_2 - G_1)}\right\} / \ln(R) \qquad (16a)$$

$$G_{app} = \frac{G_{k+1} + R^n G_k}{(1 - R^n)} \qquad (16b)$$

$$B = \frac{G_{app} - G_k}{R^{n(k+1)}\, h_1^n} \qquad (16c)$$

The average error over all grid points can be calculated from Eqs 15a through 15c. For predicted average Nusselt number for these different grid spacing (6X6 , 12X12 and 24X24), the overall errors are 44.7% , 30.9% and 4.5% respectively between approximate and numerical solutions.

4- Results and Discussions

Figure 3 shows steady-state stream function and temperature patterns for Pr=0.71 and $Ra=10^4$. The position of the isothermal lines is unrealistic. This is due to the lighter fluid lies below the heavier fluid at some positions of the cavity. This position is happend due to that the values of the coefficients C_1 and C_2 are changed from boundaries to the centre of cavity for calculating time steps of the energy, stream function and vorticity equations.

Figure 4 shows transient stream function and temperature patterns at different time intervals for Pr=0.71 and $Ra=10^4$. The position of isothermal lines is realistic. This is due to that the density of molecules of the fluid neighboring the hot side decreases. Then the fluid inside the cavity will move upward. At the cold side, the density of the fluid increases, then the fluid descends. This position happens due to that the coefficients of second derivative terms are kept constant for calculating time steps of energy and stream function equations and are changed for calculating time step of vorticity equation. Immediately, after time equal to zero the fluid bordering each side wall is motionless. this means that near the side wall the energy equation expresses a balance between thermal inertia and conduction normal to the wall. As time increases, the convection effect increases, while the effect of inertia decreases in importance. There comes a final time when a balance between the heat conducted from the wall and the enthalpy carried away vertically by the buoyant layer, as well as, a momentum balance between buoyancy and viscous diffusion. Initially two streamline cells appear near the vertical walls due to the buoyancy force. The flow in the cavity may be characterized by two periods. The first period is the transition region where there is significant heat transfer across the center of the cavity by conduction as shown in Fig. (4-a). The second period is the fully developed period where the transport mechanism is eddy diffusion across the center of cavity as shown in Fig. (4-d). The transient position shows two convection roils which are growing into the core region. As the time progresses, the buoyancy effects become significant, the roils move toward the center and two convection roils disappear into one roil.

Figure 5 shows steady state stream function and isothermal patterns for tall cavity (A=2) of $Ra=10^4$ and Pr=0.71. The temperature difference between the isothermal is 0.1. For the tall cavity, natural convection needs higher

Rayleigh number to begin than square cavity. However, for the shallow cavity which shown in Fig. 6, natural convection needs smaller value of Rayleigh number to begin than square cavity. As a result of the natural convection in the fluid, the isotherms at the left vertical side shows opposite trend to the one at the right vertical side .

Figure 7 shows the effect of Rayleigh number on the average Nusselt number with different aspect ratio for Pr=0.71. As Rayleigh number increases, average Nusselt number increases at a certain value of aspect ratio. As aspect ratio increases from 1 to 2, high temperature difference is needed to begin the current of natural convection as

$$\overline{Nu}=0.137\ Ra^{0.246}\ , \qquad 5\chi10^3 \le Ra \le 10^6\ , \quad Pr=0.71\ , \quad A=2. \qquad (17)$$

This is due to the fact that the vertical boundary layer regime is converted into talls system regime. Vertical thermal boundary layers form distinctly along the differentially heated side walls. The heat transfer rate across the cavity scales is $(k/\delta)\ H\ \Delta T$ as shown in fig. (5). The present correlation for aspect ratio equal to 1 is

$$\overline{NU}= 0.132\ Ra^{0.308}\ , \qquad 10^3 \le Ra \le 10^6. \qquad (18)$$

For most of the cavity height , the temperature varies linearly between the two side walls .i. e The heat is transferred in one dimension. The heat transfer rate is of order $KH\Delta T/ L$. The present work is *in* good agreement with previously published work as shown in Table (1).

Figure(8) shows the effect of aspect ratio on the average Nusselt number at different Rayleigh number for Pr=0.71. As the aspect ratio decreases, the average Nusselt number increases. The convection current in this case of shallow enclosure is dominant at small value of Rayleigh number than that of the square enclosure. The present correlation for the aspect ratio between 0.5 and 0.9 is

$$\overline{Nu}= 1 + 0.5598\ \left(\frac{1}{A}\right)^{0.049}\ \left(\frac{Ra}{1000}\right)^{0.49} \qquad (19)$$

with

$$10^3 \le Ra \le 10^6$$
$$0.5 \le A \le 0.9$$

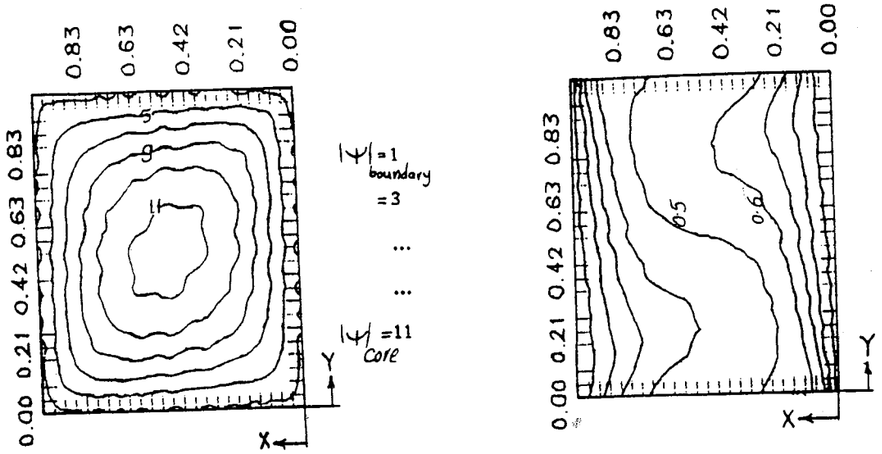

Fig.(3): Steady-state stream function and isothermal patterns for Pr=0.71 and $Ra=10^4$, A=1.

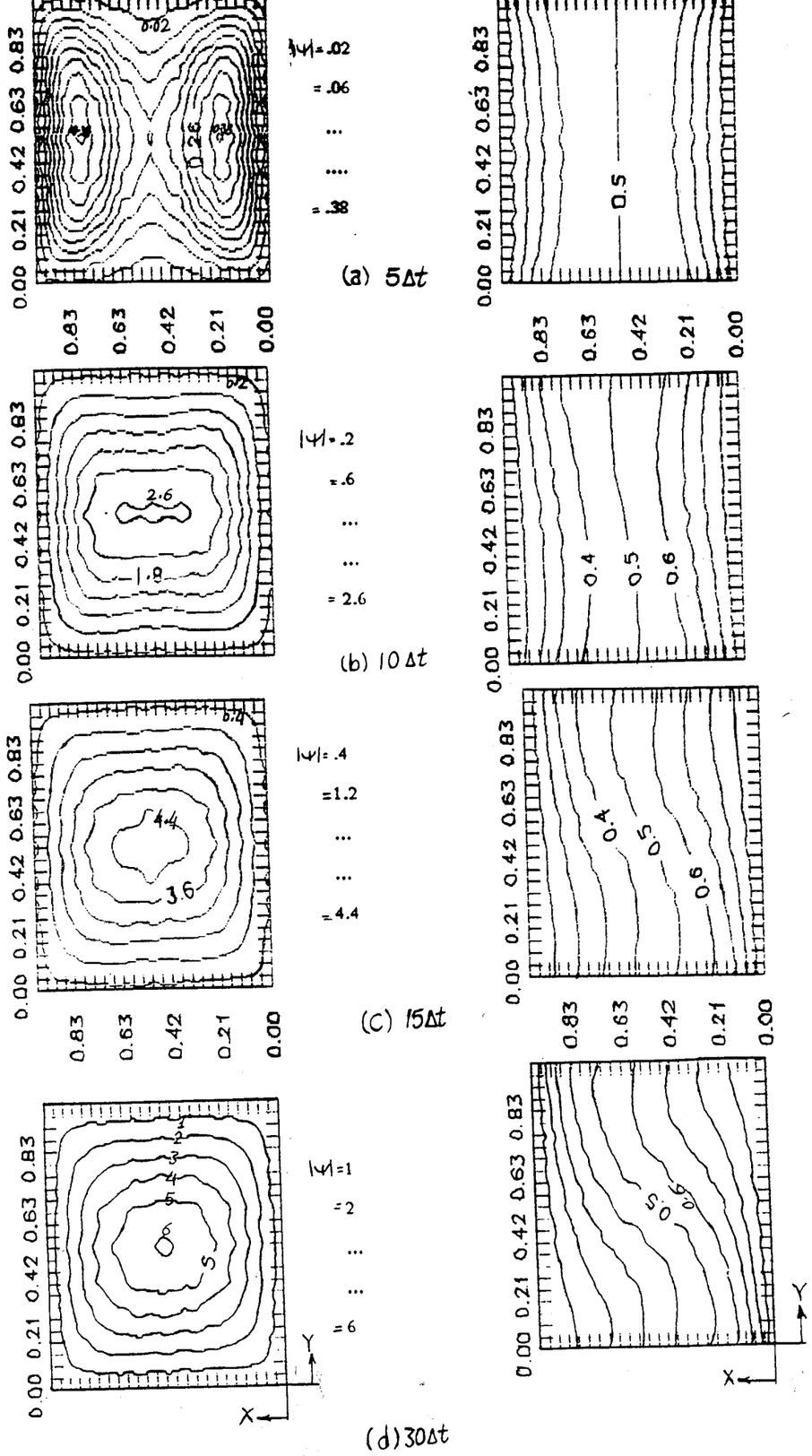

Fig.(4): Transient stream function and isothermal patterns at different time intervals for Pr=0.71 and $Ra=10^4$, A=1.

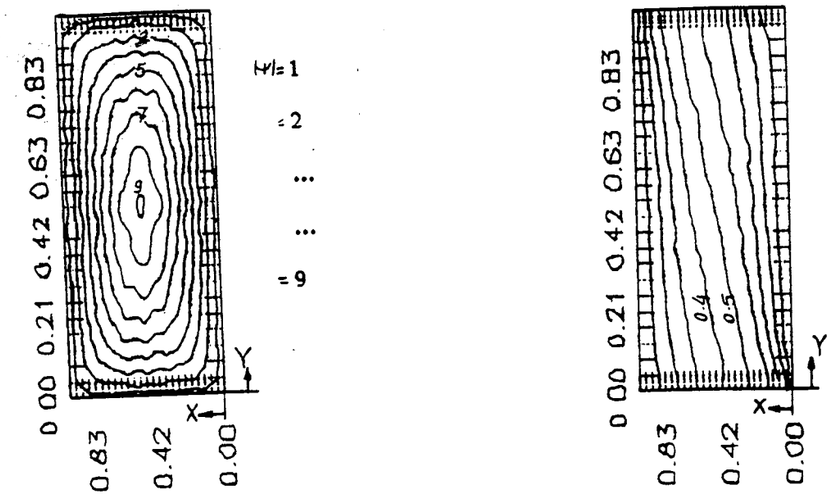

Fig.(5): Steady-state stream function and isothermal patterns for Pr=0.71 and $Ra=10^4$, A=2.

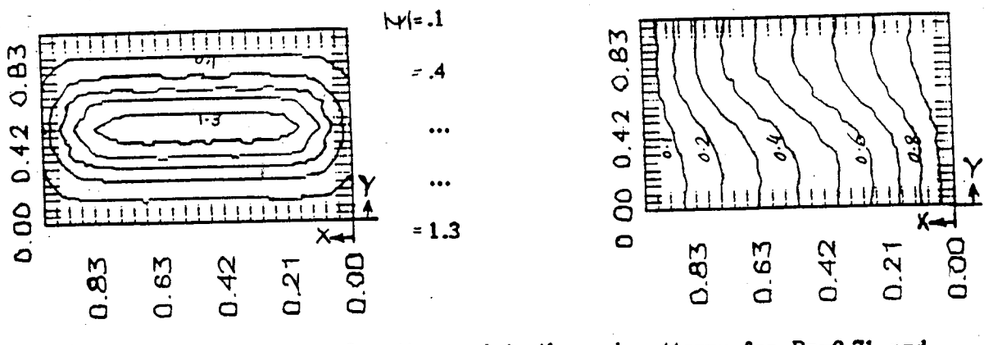

Fig.(6): Steady-state stream function and isothermal patterns for Pr=0.71 and $Ra=10^4$, A=0.5.

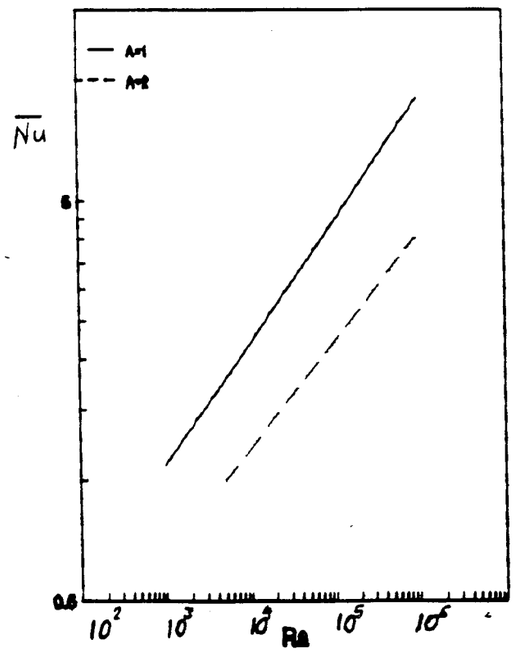

Fig.(7): Effect of Rayleigh number on the average Nusselt number at different aspect ratio ,Pr=0.71

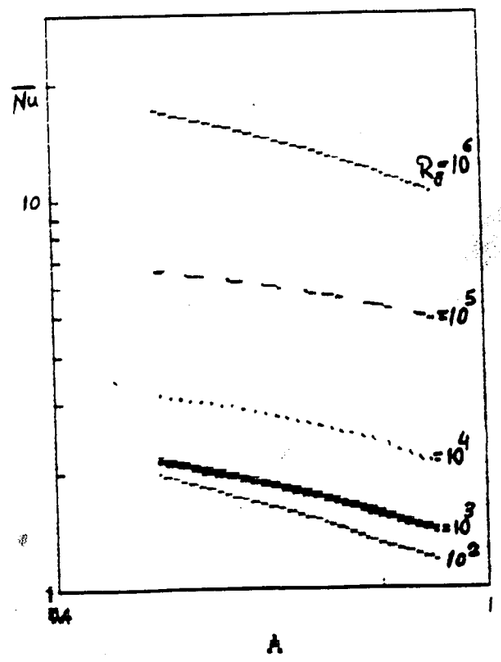

Fig.(8): Effect of aspect ratio on the average Nusselt number at different Rayleigh number , Pr=0.71

Table 1 : Comparison of average Nusselt numbers between present and published results for a square cavity at different Rayleigh numbers , Pr = 0.71

work of	Nu					
Ra	10^3	10^4	10^5	10^6	10^7	10^8
Lauriat [8]	1.120	2.268	4.623	9.330	-----	-----
Shralkar and Tien [9]	1.131	2.277	4.687	9.012	-----	-----
De Val Davis [10]	-----	-----	4.517	8.798	-----	-----
Abrous and Emery [11]	-----	-----	4.584	9.052	16.18	32.84
Breton et al [12]	-----	-----	4.521	8.794	16.38	29.39
Present result	1.120	2.260	4.530	9.010	16.15	29.71

5-Conclusions

Test computer runs have shown that the computation time necessary to simulate free convection in closed container of moderate size (volume $1m^3$) over a time period of approximately 5 days is somewhat below 1hour. The resulting implicit method is stable up to a Rayleigh number of 10^{12}. This is essentially due to the use of the method of second upwind differencing. However , it should be kept in mind that the present method is restricted to laminar flow. Computational time step is an important parameter which affects on the natural convection in cavities . The current of natural convection depends upon the value of aspect ratio and Rayleigh number . The flow in a laminar boundary layer regime can be characterized by two distinct regions (a) the transition region where there is significant heat transfer across the centre of the enclosure by conduction (b) the fully developed region where the transport mechanism is eddy diffusion across the centre of the enclosure . Correlations for the tall, square and shallow cavities are obtained for a certain range of Rayleigh number and aspect ratio.

Nomenclature

A	aspect ratio
A_x, A_y, B_x, B_y	derivatives of the transformation equation
$\frac{d}{dt}$	total differential
g	gravity
H	height of the cavity
I	grid point notation in y-direction
J	grid point notation in x-direction
L	width of the cavity
Nu	local Nusselt number (Eq. 18)
Pr	Prandtl number ($=\frac{\nu}{\alpha}$)
p	pressure
q(y), r(x)	transformation relation
Ra	Rayleigh number ($=\frac{g\,\beta\,\Delta T\,L^3}{\nu\,\alpha}$)
t	time
T	temperature
U=(u,v)	velocity
U,V	dimensionless velocities in X and Y directions
Uo	reference velocity
X	dimensionless horizontal coordinate
Y	dimensionless vertical coordinate
Greek symbols	
α	thermal diffusivity
Γ	dummy variable
Θ	dimensionless temperature $\frac{T - T_c}{T_h - T_c}$
ρ	density

Subscripts

c	cold
h	hot
o	initial value
r	right
l	left

ν	kinematic viscosity
τ	dimensionless time (Fourier number)
ψ	stream function
ω	vorticity
Ψ	dimensionless stream function ($=\frac{\psi}{U_0 L}$)
Ω	dimensionless vorticity($=\frac{\omega L}{U0}$)
∇	nabla operator
∇^2	Lablace operator
ϵ	convergence criterion
δ	thermal boundary layer thickness

REFERENCES

1- Moog, W., Theoretical considerations of similarity for air flow within the open space, Klima Kalteingenieur, Jg. 6, Heft 11, 1978

2- Torrence, K. E., Comparison of finite element computation of natural convection, J. Res., NBS 72B, 1968.

3- Roache, P. J., Computational Fluid Dynamics, Hermosa, Albuquerque, U.S.A., 1976.

4- Patankar, S. V., Numerical Heat Transfer and Fluid Flow, McGraw-Hill Book Co., NewYork, 1980.

5- Bejan, A., Convection Heat Transfer, John Wiley and Sons, NewYork, 1984

6- White, F. M., Viscous Fluid Flow, McGraw-Hill, NewYork, 1974

7- Peaceman D. W. and Rachford, H. H., The Numerical Solution of Parabolic and Elliptic Differential equations, J. Soc. Indust. appl. Math. 3(1), 28-41, 1955.

8- Lauriat, G., Natural Convection in an Enclosd Cavity : A Comparison Problem", in Numerical Solutions for a Comparison Problem on Natural Convection in an Enclosed Cavity, Edited by Jones, I. P. and Thmpson, C. P., AERE-R9955, IIMSO, pp. 89-91, 1981

9- Shralkar G. S. and Tien, C., A Numerical Study of the Effect of a Vertical Difference Imposed on a Horizontal Enclosure, Numerical Heat Transfer, Vol. 5, pp. 185-197, 1981.

10- De Vahl Davis, G., Natural Convection of Air in a Square Cavity: A Bench Mark Numerical Solution, International Journal of Numerical Methods in Fluids, Vol. XX, pp. 227-248., 1983

11- Abrous A. and Emery, A. F., Turbulent Free Convection in Square Cavities Flows, ASME, HTD-Vol. 107, 1989.

12- Le Breton, P., Caltagirone J. P. and Arquis, E., Natural Convection in a Square Cavity With Thin Porous Layers on its Vertical Walls, ASME, J. of Heat Transfer, Vol. 113, pp.892-898, 1991